

Applicability of Shape Memory Alloy Wire for an Active, Soft Orthotic

Leia Stirling, Chih-Han Yu, Jason Miller, Elliot Hawkes, Robert Wood, Eugene Goldfield, and Radhika Nagpal

(Submitted April 9, 2010; in revised form January 18, 2011)

Current treatments for gait pathologies associated with neuromuscular disorders may employ a passive, rigid brace. While these provide certain benefits, they can also cause muscle atrophy. In this study, we examined NiTi shape memory alloy (SMA) wires that were annealed into springs to develop an active, soft orthotic (ASO) for the knee. Actively controlled SMA springs may provide variable assistances depending on factors such as when, during the gait cycle, the springs are activated; ongoing muscle activity level; and needs of the wearer. Unlike a passive brace, an active orthotic may provide individualized control, assisting the muscles so that they may be used more appropriately, and possibly leading to a re-education of the neuro-motor system and eventual independence from the orthotic system. A prototype was tested on a suspended, robotic leg to simulate the swing phase of a typical gait. The total deflection generated by the orthotic depended on the knee angle and the total number of actuators triggered, with a max deflection of 35°. While SMA wires have a high energy density, they require a significant amount of power. Furthermore, the loaded SMA spring response times were much longer than the natural frequency of an average gait for the power conditions tested. While the SMA wires are not appropriate for correction of gait pathologies as currently implemented, the ability to have a soft, actuated material could be appropriate for slower timescale applications.

Keywords gait, orthotic, shape memory alloy springs

1. Introduction

Current treatments for gait pathologies associated with neuromuscular disorders (such as drop-foot, spasticity, etc.) may include use of a passive mechanical brace (Ref 1). Depending on the severity of the gait pathology, the brace may be applied at the hip, knee, ankle, or any combination of these joints to improve balance and gait.

While passive mechanical braces provide certain benefits, they may also lead to additional medical problems. For example, in the case of drop-foot, an ankle foot orthotic (AFO) is typically used to prevent the toe from dragging on the

ground. Rigid versions of the AFO constrain the ankle to a specific position, while hinged or flexible versions of the AFO allow limited flexion. Limiting the range of ankle motion ensures that the toe clears the ground, thus allowing gait to progress more naturally. However, the use of the AFO may result in a reduction in power generation at the ankle, as it limits active plantar flexion. Rigid versions of the AFO may lead to disuse atrophy of the muscles, such as the tibialis anterior muscle, potentially leading to long-term dependence (Ref 2). Models designed to allow increased mobility, such as leaf spring AFOs, will break if they are too flexible, but limit motion if they are too stiff. These limitations of AFOs make it clear that the amount of flexibility should be patient-specific, specifically taking pathological conditions into account. Morris (Ref 3) points out that children with less severe impairments often performed better in conditions such as climbing stairs or controlling perturbed balance when wearing less-restrictive designs.

DM Orthotics, Ltd. has examined passive flexible architectures using Lycra[®] specially designed according to the assistive needs of each child. Studies have shown this to be helpful for children with cerebral palsy in cases such as eliminating flexed walking patterns (Ref 4). One limitation to these designs is that as the child ages or requires varied assistance, the Lycra[®] orthotic must be redesigned and fit as the support is entirely passive and based on the layers of reinforcement placed within the material.

While previous researchers have incorporated actuation into rigid orthotics (Ref 5), we introduce a novel approach for embedding actuation within a soft material to create an active, soft orthotic (ASO). In this manner, the orthotic may provide variable assistance as a function of location of the limb during the gait cycle, activity level, and movement limitations of the wearer. In this article, we present the first step in our vision of

This article is an invited paper selected from presentations at Shape Memory and Superelastic Technologies 2010, held May 16-20, 2010, in Pacific Grove, California, and has been expanded from the original presentation.

Leia Stirling, Wyss Institute, Harvard University, 5th Floor CLSB, 3 Blackfan Circle, Boston, MA 02115; **Chih-Han Yu**, **Jason Miller**, and **Elliot Hawkes**, Wyss Institute and the School of Engineering and Applied Sciences, Harvard University, 5th Floor CLSB, 3 Blackfan Circle, Boston, MA 02115; **Robert Wood**, Wyss Institute and the School of Engineering and Applied Sciences, Harvard University, 4th Floor, 60 Oxford Street, Cambridge, MA 02138; **Eugene Goldfield**, Wyss Institute, Harvard University and Children's Hospital Boston, 5th Floor CLSB, 3 Blackfan Circle, Boston, MA 02115; and **Radhika Nagpal**, Wyss Institute and School of Engineering and Applied Sciences, Harvard University, 235 Maxwell Dworkin, 33 Oxford Street, Cambridge, MA 02138. Contact e-mail: leia.stirling@wyss.harvard.edu.

an ASO: development of a robotic leg for testing the orthotic and the use of NiTi shape memory alloy (SMA) wires for actuation. There are many examples of SMA wires for generating motion in the field of prosthetic grasping including studies by Dollar and Howe (Ref 6) and O'Toole et al. (Ref 7). Implementation of SMA in lower limb orthotics is less studied, although Pittaccio and Viscuso (Ref 8) examined implementation of NiTi wire in a rigid ankle foot orthotic for stroke rehabilitation.

Our design is specifically oriented toward *individualized control*, promoting more appropriate use of the muscles, potentially enabling a re-education of the neuro-motor system, and eventually allowing a patient to perform a more typical gait while being entirely free of the orthotic system. Our specific focus at this stage of device development is the swing phase of gait, so that we may eliminate the effects of ground contact forces as well as the requirement for controlling balance.

2. Robotic Leg Test Bed

A suspended, compliant robotic leg was constructed as a test-bed for studying the ASO during the swing phase of gait. The robotic upper leg, lower leg, and foot were designed such that they were comparable to the weight and dimensions of a typical 4-year-old child (Table 1). These data were based upon values from the Generator of Body Data (GEBOD), software developed by Wright Patterson Air Force Base (Ref 9, 10). Certain design requirements resulted in values for the constructed leg to slightly differ from the body data. While leg lengths were shortened for segments to accommodate the motor, the total lower leg length became slightly longer than the average leg length due to the final motor configuration, as did the mass of the foot. However, these values are still within the range of values measured in this age group (Ref 11).

A compliant knee joint was designed such that a primary knee flexion could be set by a motor, with an additional deflection of 30° (flexion or extension) permitted by a spring. This allowed us to more closely approximate a biological leg, as the additional elasticity is similar to biological muscle and tendons, although the body's elasticity is variable due to a person's muscle tone and level of muscle co-contraction. To achieve the desired additional deflection, a rotational series elastic actuator was built that contains a torsional spring located between the motor and the output. The level of compliance was set by the stiffness of the selected spring. We designed the rotational series elastic actuator with a DC motor (Fig. 1). This

Table 1 Robotic leg and 50th percentile 4-year-old parameters

| Measurement | Robot leg value | 4-Year-old child value |
|---------------------|-----------------|------------------------|
| Upper leg length | 0.33 m | 0.33 m |
| Thigh circumference | 0.31 m | 0.32 m |
| Upper leg mass | 1.28 kg | 1.49 kg |
| Lower leg length | 0.35 m | 0.29 m |
| Calf circumference | 0.22 m | 0.22 m |
| Lower leg mass | 0.70 kg | 0.72 kg |
| Foot length | 0.16 m | 0.16 m |
| Foot breadth | 0.07 m | 0.07 m |
| Foot mass | 0.31 kg | 0.21 kg |

design is an extension of more typical translational series elastic actuators (Ref 12, 13). The ankle joint was an unactuated universal joint that permitted flexion and pronation/supination.

3. Shape Memory Alloy Orthotic

The SMA selected for the ASO was cold-worked, as-drawn Nitinol wire from Dynalloy. This wire does not exhibit shape memory properties until annealed, but because a coil was needed, custom annealing was necessary. When compared to re-annealed off-the-shelf Flexinol wire, custom-annealed as-drawn wire is an order of magnitude less expensive, has larger deflection for a given force and spring shape, and allows for greater parameter variation through choice of annealing temperature (Ref 14). The SMA selected was 0.25-mm-diameter wire wound into springs with an inner diameter of 0.51 mm. By winding the SMA wire into springs and annealing at 400 °C (no subsequent surface finishing), we increase the available strain (Ref 15) allowing for the full knee range of motion. However, by increasing the available strain, we also decrease the force that can be generated. Trading off stress for strain is achieved by choice of wire diameter and spring pitch. A 2.0-cm-long sample coil was characterized in the austenite and martensite states under load (Fig. 2). External forces were applied by hanging different weights. To minimize dynamic effects, the weights were applied very slowly. A fixed current of 500 mA was used to trigger the phase transition to the austenite state through Joule heating. Measurements for both states were made

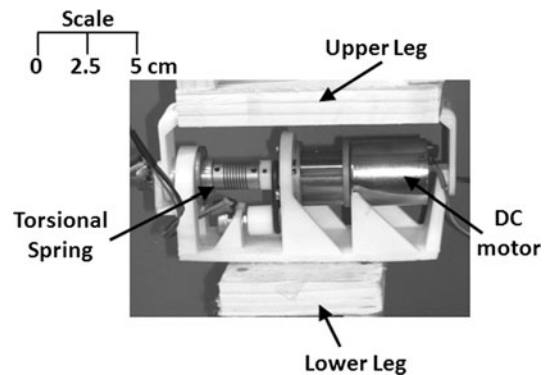


Fig. 1 Rotational series elastic actuator comprised of a DC motor and torsional spring

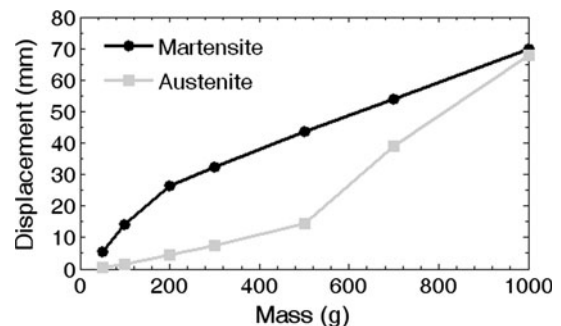


Fig. 2 Deflection of the 20-mm spring annealed at 400 °C under load

before and after the coil was loaded, with current applied before loading to transition to the austenite state. For the masses tested, detwinning occurs rapidly in the martensite coil, as seen in the steep slope for masses below 200 g. Once detwinned, the coil becomes stiffer, which is apparent in the decreased slope of the martensite curve for masses above 200 g. The austenite curve has a decreased slope compared to the detwinned martensite for masses less than 500 g, which is consistent as austenite's modulus of elasticity is higher than that of martensite. Since the stress-induced martensitic transformation follows the Clausius-Clapeyron relationship, the transition temperature can increase above the temperature the current is generating. Thus, the percentage of martensite in the heated coil increases until it is almost 100% martensite, as is the case with the applied 1000 g mass. The effective stroke length of the coil for the fixed 500 mA current can be estimated by differencing the displacement of the coil in the martensite state with the value in the austenite state for a given mass.

The ASO for the knee comprised four sets of actuators on the dorsal surface of the knee (to assist flexion), and one set on the frontal surface (to assist extension), as seen in Fig. 3(a). The nominal (unstretched) length of the actuators was 17.5 cm for the front and back of the leg. The ASO for the ankle consisted of four sets of actuators, with one set on the frontal surface (to assist dorsiflexion), one set on the dorsal surface (to assist plantar flexion), and one set on each lateral surface (to assist pronation and supination), as seen in Fig. 3(b). Each actuator

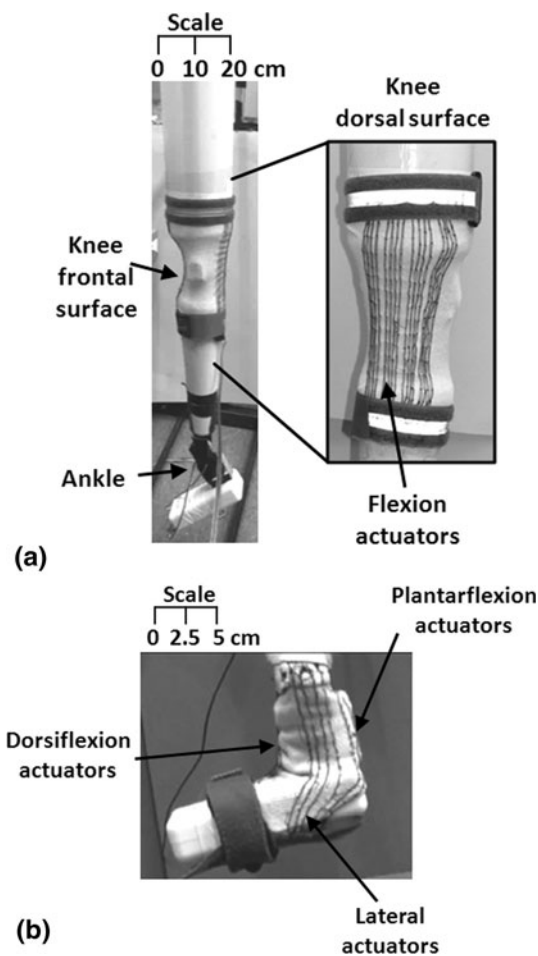


Fig. 3 The robotic leg with the ASO for the (a) knee and (b) ankle

set consisted of four lines of the SMA coils. The top and bottom of the orthotic were coated with silicone to prevent the orthotic from slipping on the robotic leg.

The orthotics were controlled in a binary fashion by passing current through the springs to trigger a phase transition via Joule heating. No intermediate states were configured. However, each actuator could be triggered individually, allowing for selective actuation, similar to biological muscle recruitment. During testing, the orthotics were tethered to an external power source and angle measurements of the knee were made using a goniometer (PASCO, Roseville, CA).

4. Results and Discussion

Experiments were run to characterize the knee orthotic performance, including the actuation response time, the total deflection of the knee, and the effect of varying initial knee angles. For this stage of development, we obtained only qualitative measures of ankle ASO performance. For all tests, the motors and actuators were powered externally by a standard power supply.

When all four flexion sets for the knee were actuated with the motor off, the total steady-state deflection was approximately 34° (Fig. 4a), which would permit a significant assist during the swing phase of gait. However, the response time to reach steady state was about 25 s, which would be too long for an immediate gait assist device (a typical gait has a natural frequency around 1 Hz). However, the speed of actuation is a function of the applied load and the electric current, which will be discussed shortly. Based on these results, intermediate angles could be reached more quickly, or quasi-static control could be implemented, which adapts every few steps. Note that even though the power of the motor was off, its effect on the resulting motion is evident in the temporary plateau regions of the curve before reaching the steady state knee angle. As the actuators cause the knee to bend, the motor passively goes through its range of motion. Although the DC motor does not have an integrated gearbox, there is still friction within the system, which is a function of velocity, applied force, and motor orientation. This friction causes the decreased rate of knee deflection, resulting in the temporary plateaus.

When the DC motor was turned on and set to hold the knee at a specific value (18°), the largest contribution to the deflection could be achieved with two sets of actuators (Fig. 4b). As seen in Table 2, the increase from one actuator set to two actuator sets more than tripled the response rate and provided an additional 15.7° of deflection. Increasing to three actuator sets provided an additional 4.1° of deflection and achieved a response rate increase of 38%. However, adding the fourth set of actuators provided only an additional 3.1° of deflection and did not further increase the response rate. By having the DC motor on and fixed at a specific position, the backdrive ability is limited. Thus, the motion obtained is due to the deflection of the torsional spring in the knee.

The deflection made possible by the orthotic was also affected by the initial knee angle (Fig. 5a). As the DC motor hold angle was increased, a decrease in net knee flexion is observed. First, recall that the knee was designed to permit approximately 30° of additional flexion. At hold angles of 0° and 11° , an additional flexion of 30° was observed. At hold angles of 27° , 41° , and 45° , additional flexions of 21° , 10° , and

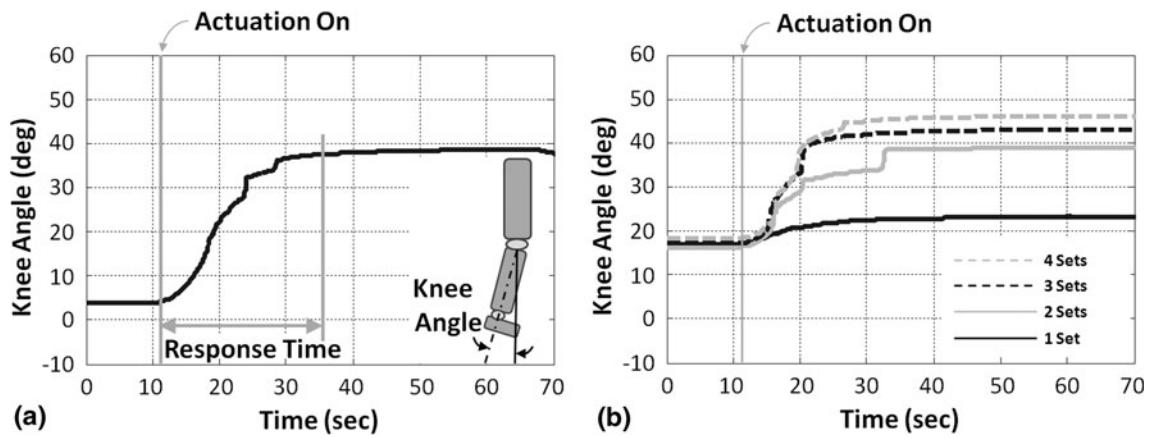


Fig. 4 (a) All flexion actuator sets triggered simultaneously with the DC motor inactive. (b) Effect of triggering different numbers of flexion actuators with the DC motor active and holding at 18° of flexion

Table 2 Effect of the number of actuators on the robotic knee deflection

| Number of actuator sets | Final knee flexion, ° | Percent total, % | Response rate, %/s |
|-------------------------|-----------------------|------------------|----------------------|
| 1 | 23.3 | 50.4 | 0.51 ($r = 0.996$) |
| 2 | 39.0 | 84.4 | 1.88 ($r = 0.974$) |
| 3 | 43.1 | 93.5 | 2.56 ($r = 0.980$) |
| 4 | 46.2 | 100 | 2.56 ($r = 0.966$) |

9°, respectively, were observed. At the larger hold angles, only a portion of the compliance is used in the knee. By further increasing the hold angle, we would be able to determine the limit where no additional rotation is achieved. The decrease in additional flexion can be better understood by considering a schematic of the forces and moments on the system (Fig. 5b). As the knee flexion is increased, the effective force due to gravity increases. (Recall the effective force is the component perpendicular to the line of action, as the force applied parallel to the line of action does not produce a torque.) This implies that as the knee flexion increases, the torque due to gravity increases. Now consider the forces due to the SMA on the knee. Neglecting losses in force due to fabric deformation and assuming the force applied is not affecting the material

properties of the SMA, the effective force applied by the SMA can be considered constant. Thus, the torque generated by the SMA stays the same, and the torque due to gravity increases due to increasing knee flexion, causing the reduction in net flexion.

Another key consideration for the evaluation of the ASO is power consumption: ideally the ASO would be self-contained, allowing the user to operate without the need of a tether. For these tests, we limited the maximum voltage to 18 V, yielding a current of 0.4 A for each of the four actuator sets. These conditions lead to a total consumption of 28.8 W. A Lithium Polymer battery rated at 6 Ah with nominal voltage of 3.7 V would need a boost converter to achieve the 18-V requirement. Typically, increasing the voltage by this factor would reduce the overall efficiency of the system. If we use a Maxim MAX668/669 series converter operating with these specifications, then we would expect 85-90% efficiency according to the technical documentation. Thus, assuming the lower end value of 85% would lead to the battery providing 18.9 W h. If we assume the knee ASO is used for only one leg, and is signaling all four flexion actuator sets to be powered during swing, (approximately 40% of the gait cycle; (Ref 16)), the battery could potentially yield a continuous operation time of around 1.1 h. However, if the actuators need to be powered throughout the entire gait cycle, as when using a quasi-static control, then the battery could only yield a continuous operation time of around

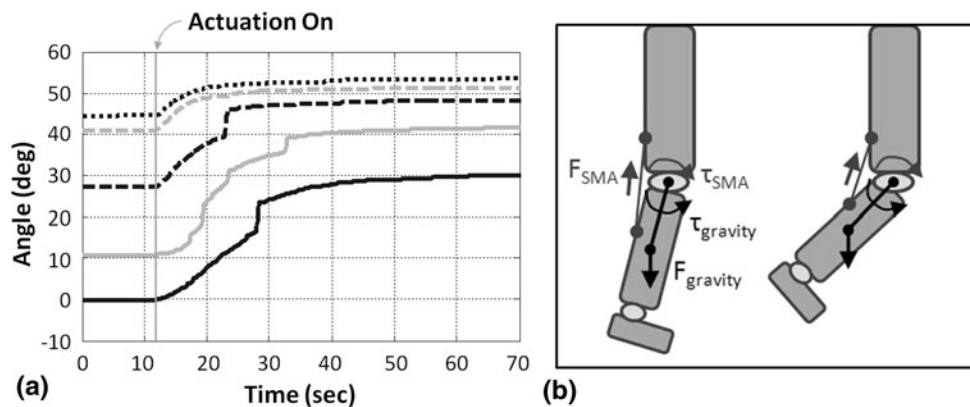


Fig. 5 (a) Effect of varying the starting angle with all flexion actuator sets triggered simultaneously. (b) Schematic of the forces and moments about the knee due to the SMA (F_{SMA} , τ_{SMA}) and due to gravity ($F_{gravity}$, $\tau_{gravity}$). The increased knee angle causes a greater $\tau_{gravity}$, resulting in a reduction in net deflection

39 min. These times assume that the losses from other components are minimal and that no other actuation sets are needed. If we include the set of actuators to assist in knee extension, as well as the sets that assist the ankle, then we would see the battery life decrease even further. Had we increased the maximum voltage to obtain a higher current necessary for a faster response time, we would not only see our battery life affected (or the need for additional batteries), but we would have to weigh the effects of consumer safety in the design of a high-voltage, high-current system.

A concern for designers using SMA is not only the activation times, but the cooling times. Natural convection would be an insufficient method for cooling the SMA actuators within the knee ASO as cooling times were on the order of 40–50 s for the trials presented in Fig. 4 and 5. Thus, a forced cooling of the SMA actuators would be required for any real-time implementation. Although not investigated here, forced cooling has been examined in other studies using methods such as heat sinking (Ref 7, 17) and forced air or water convection (Ref 18, 19).

5. Conclusions

While the SMA springs provide the ability to embed actuators into a soft material, we discovered several design challenges. Here, with a custom-designed robotic leg, we found that the response time was too slow for control during each step of a simulated gait cycle for the selected design choices. While the SMA spring actuators made possible a full range of knee motion, they brought along a reduction in the generated force, which added to the increase in response time. While future efforts could focus on optimizing the spring parameters and attachment points to achieve the necessary strain with an increased force production, this early study highlights the significant power needed to operate the actuators. Although SMA wires provide a large energy density, they would be difficult to use for actuation for a full day when not tethered to an external power supply. The power required could be mitigated by decreasing the number of actuators; however, this would also have to be balanced with an increase in force production of the individual wires. For this application, the SMA may not be appropriate; however, the ability to have a soft, active material has promise in applications with slower time scales, or reduced forces.

Acknowledgment

This research has been funded by the Wyss Institute at Harvard University.

References

1. F. Miller, *Cerebral Palsy*, Springer, New York, NY, 2005
2. S. Hesse, C. Werner, K. Matthias, K. Stephen, and M. Berteau, Non-Velocity-Related Effects of a Rigid Double-Stopped Ankle-Foot Orthosis on Gait and Lower Limb Muscle Activity of Hemiparetic Subjects with an Equinovarus Deformity, *Stroke*, 1999, **30**(9), p 1855–1861
3. C. Morris, A Review of the Efficacy of Lower-Limb Orthoses Used for Cerebral Palsy, *Dev. Med. Child Neurol.*, 2002, **44**(3), p 205–211
4. M. Matthews, M. Watson, and G. Richardson, Effects of Dynamic Elastomeric Fabric Orthoses on Children with Cerebral Palsy, *J. Prosthet. Orthot. Int.*, 2009, **33**(4), p 339–347
5. J. Blaya and H. Herr, Adaptive Control of a Variable-Impedance Ankle-Foot Orthosis to Assist Drop-Foot Gait, *IEEE Trans. Neural Syst. Rehabil. Eng.*, 2004, **12**(1), p 24–31
6. A. Dollar and R. Howe, The Highly Adaptive SDM Hand: Design and Performance Evaluation, *Int. J. Robot. Res.*, 2010, **29**(5), p 585–597
7. K. O'Toole, M. McGrath, and E. Coyle, Analysis and Evaluation of the Dynamic Performance of SMA Actuators for Prosthetic Hand Design, *J. Mater. Eng. Perform.*, 2009, **18**(5–6), p 781–786
8. S. Pittaccio and S. Viscuso, An EMG-Controlled SMA Device for the Rehabilitation of the Ankle Joint in Post-Acute Stroke, *Proceedings of the International Organization on Shape Memory and Superelastic Technologies*, 16–20 May, 2010, p 40–41
9. H. Cheng, L. Obergefell, and A. Rizer, “Generator of Body Data (GEBOD), Manual,” AL/CF-TR-1994-0051, Wright-Patterson AFB, OH, March 1994
10. H. Cheng, L. Obergefell, and A. Rizer, The Development of the GEBOD Program, *Proceedings of the Fifteenth Southern Biomedical Engineering Conference*, 1996, p 251–254
11. R. Snyder, L. Schneider, C. Owings, H. Reynolds, H. Golomb, and A. Schork, “Anthropometry of Infants, Children, and Youths to Age 18 for Product Safety Design,” UM-HSRI-77-17, Bethesda, MD, May 1977
12. J. Pratt, B. Krupp, and C. Morse, Series Elastic Actuators for High Fidelity Force Control, *Ind. Robot*, 2002, **29**(3), p 234–241
13. G. Pratt and M. Williamson, Series Elastic Actuators, *Proceedings of the IEEE International Conference on Intelligent Robots and Systems*, Vol 1, 1995, p 399–406
14. S. Kim, E. Hawkes, K. Cho, M. Jolda, J. Foley, and R. Wood, Micro Artificial Muscle Fiber Using NiTi Spring for Soft Robotics, *Proceedings of the IEEE/RSJ International Conference on Intelligent Robots and Systems*, 11–15 October 2009, p 2228–2234
15. K. Cho, E. Hawkes, C. Quinn, and R. Wood, A Design, Fabrication and Analysis of a Body-Caudal Fin Propulsion System for a Microrobotic Fish, *Proceedings of the IEEE International Conference on Robotics and Automation*, 19–23 May 2008, p 706–711
16. M. Murray, P. Drought, and R. Kory, Walking Patterns of Normal Men, *J. Bone Joint Surg.*, 1964, **46**(2), p 335–360
17. M. Gharaybeh and G. Burdea, Investigation of a Shape Memory Alloy Actuator for Dexterous Force-Feedback Masters, *Adv. Robot.*, 1995, **9**(3), p 317–329
18. G. Webb, L. Wilson, D. Lagoudas, and O. Rediniotis, Adaptive Control of Shape Memory Alloy Actuators for Underwater Biomimetic Applications, *AIAA J.*, 2000, **38**(2), p 325–334
19. P. Wellman, W. Peine, G. Favalora, and R. Howe, Mechanical Design and Control of a High-Bandwidth Shape Memory Alloy Tactile Display, *Exp. Robot. V*, 1998, **232**, p 56–66